Physicochem. Probl. Miner. Process., 55(6), 2019, 1475-1483

http://www.journalssystem.com/ppmp

Physicochemical Problems of Mineral Processing

ISSN 1643-1049
© Wroclaw University of Science and Technology

Received July 30, 2019; reviewed; accepted October 4, 2019

Synthesis and selected physicochemical properties of hydroxyapatite and white clay composite

Ewa Broda [1], Ewa Skwarek [1], Victoria V. Payentko [2], Vladimir M. Gunko [2]

[1] Faculty of Chemistry, Maria Curie-Skłodowska University, Maria Curie-Skłodowska Sq. 3, PL-20031 Lublin, Poland

[2] Chuiko Institute of Surface Chemistry, 17 General Naumov Street, 03164 Kyiv, Ukraine

Corresponding author: ewunias@hektor.umcs.lublin.pl (Ewa Skwarek)

Abstract: Hydroxyapatite (HAP) composites are very important biomaterials, which can be applied in various life areas. HAP composite with white clay was prepared and studied using X-ray diffraction, nitrogen adsorption, Fourier transform infrared spectroscopy (FTIR), potentiometric titration, and quasi-elastic light scattering and zeta potential measurements. The values of pH_{pzc} (point of zero charge) and pH_{IEP} (isoelectric point) which characterize the electrical double layer depend strongly on the white clay addition to HAP. Comparative studies of hydroxyapatite, white clay and composite using nitrogen adsorption and FTIR methods showed that in most cases composite has the properties nearly intermediate between hydroxyapatite and white clay taken for the synthesis; however, certain non-additivity was observed analyzing the properties, due to precipitation of HAP onto clay particles that changes the HAP formation conditions in comparison to HAP formation alone. Thus, changes in the condition of the composite preparation allow one to control the properties of the final materials.

Keywords: hydroxyapatite, white clay, composite compounds

1. Introduction

Clays are defined as naturally occurring cheap materials, which composed mainly of fine-grained minerals used in many applications (Ehlers and Blatt, 1982; Murray, 1991; Middleton et al., 2003; Bergaya et al., 2006; Montes-Hernandez et al., 2014; Mishra et al., 2018; Zhang et al., 2019; Zhuang et al., 2019). Clays are generally plastic at appropriate water content, and will harden after drying or strong heating. Clays usually contain phyllosilicates; however, they might contain other materials, which can exhibit different properties. Clay associated phases may include organic matter and materials that do not impact plasticity. Geologists and soil scientists use term clay for particle size less than 2 μm, sedimentologists – 4 μm and colloid chemists – 1 μm. Clay plasticity is mainly affected by material chemical composition, however, influence on plasticity has also aggregate nature of the particles in the material (Guggenheim, 1995).

The process of clay minerals formation and acceleration may be caused by many different processes. Most of them, involving chemical processes and physical water movements, occur in the environment (Hillier, 2006). Three mechanisms of clay formation can be distinguished: inheritance, neoformation and transformation. Clay mineral formed by inheritance is originated from reactions occurred during rock cycle. This clay is stable in actual environment, because of slow reaction rate or chemical equilibrium. If clay is formed by precipitation from solution or as amorphous material reaction products, it is neoformation. Transformation origin means that clay keeps undisturbed structure, despite chemical reactions course. It can be ion exchange reaction or layer transformation. Determination of clay origin gives information about environmental conditions in area of clay sediment (clays formed by inheritance and transformation) or about in situ environment changes (clays formed by neoformation and transformation) (Eberl et al., 1984).

DOI: 10.5277/ppmp19073

Clay minerals occur in the Earth's crust, in ocean sediments, atmospheric aerosols. Clay determines physical and chemical properties of soil, as it is one of its basic components (Ito and Wagai, 2017). Also, kaolinite is widely spread in nature – it occurs in almost all continents, except Antarctica. White clay is rich in aluminum silicate. It is used internally in the form of an aqueous suspension and externally as an ointment, compresses, a washing agent and a mask component. White clay nourishes the skin, removes toxins and strengthens teeth.

Clay minerals are hydrated aluminum aluminosilicates (as well as magnesium and iron) with a characteristic, layered crystalline structure. One of the layers contains silicate tetrahedrons whose centers are Si^{4+}surrounded by four oxygen atoms. These tetrahedrons are connected to each other to form a hexagonal arrangement of $Si_2O_5^{2-}$ units. The second layer is formed by aluminum hydroxide octahedrons in which Al^{3+} is surrounded by six hydroxyl groups. The layers combine into characteristic systems that determine their properties and form the basis for the classification of clay minerals. The basic building blocks of clay minerals are tetrahedral silicates and octahedral hydroxide sheets. Tetrahedral and octahedral sheets arrangement divide clay minerals into various classes e.g. 1:1 or 2:1. Kaolinite is a planar hydrous aluminium phyllosilicate, which belong to the dioctahedral kaoline group 1:1, composed of one silica and one alumina layer. Kaolinite formula is $Al_2Si_2O_5(OH)_4$ (Miranda-Trevino and Coles, 2003). Very minor isomorphic substitution of silicon and aluminium result in a low charge of kaolinite layers. Two contiguous layers are linked through hydrogen bonding -Al-O-H…O-Si-. Because of series of stacking faults in the *ab* plane and along *c*-axis, poor structural order for kaolin is commonly observed. Kaolin has a tendency to form many polytypes (Kenne Dedzo and Detellier, 2017).

A special attention should be paid to hydroxyapatite which is a very important ceramic material applied in biomedicine. It is a main component of inorganic bones and teeth constituting about 70% wt. of bones and as much as 90% wt. of tooth enamel. Taking into account the fact that the adult bone system constitutes about 30% of the whole body mass, each of us contain a lot of this material. It constitutes a mineral scaffold for the connective tissue which is responsible for the mechanical strength of bones. Natural hydroxyapatite occurs mainly in sedimentary rocks. However, synthetic hydroxyapatite is the mostly exploited. Hydroxyapatite of the best physicochemical properties and high purity can be obtained by many methods which can be classified as wet (Szymański, 1991; Riman et al., 2002; Guzman et al. 2005; Suzuki et al., 1998; Dean-Mo, 1996), dry (Murugan, 2007), hydrothermal, sol-gel (Guzman et al. 2005; Sopyan et al., 2008), emulsion and those based on co-precipitation (Dean-Mo, 1996). There are also mechanochemical and from natural raw materials methods but they are not applied on a large scale (Rhee, 2002; Sobczak et al., 2009). In all methods the reagents, which are a source of calcium, phosphorus and regulate reaction pH, are used. Wet methods have become more common. The solid product obtained from such reactions is washed with redistilled water to obtain its steady conductivity and dried (Dorozhkin, 2010). The hydroxyapatite crystals obtained by this method can be amorphous or of small crystallinity degree. The advantage of the wet method is possibility of introducing sodium, magnesium, potassium ions or carbonate groups into the hydroxyapatite structure. In our studies, wet methods described in the papers were applied (Skwarek et al., 2016 and 2017; Janusz et al., 2016; Mostafa, 2005), different reagents were also used: calcium acetate $(CH_3COO)_2Ca$ and dipotassium biphosphate K_2HPO_4.

The presented investigations are of great applicative potential in many areas of pharmaceutical, cosmetic and food industries, processing of minerals and sewages, purification methods from metals. Moreover, newly obtained composites can be applied as new adsorbents. These studies describe synthesis and characteristic properties of a composite based on hydroxyapatite and white clay.

2. Materials and methods

White natural clays (commercial and certified at "Mel–OK", Kyiv, Ukraine) were used in this study (Azov region, mainly kaolinite). Di-potassium hydrogen phosphate (pure p.a.) was purchased from POCH SA, calcium acetate hydrate (pure) was purchased from Riedel-de Haën, and both were used as reagents in HAP synthesis. Into a three-necked round-bottomed flask 0.77 g of white clay and 0.2 dm^3 of redistilled water were transferred (mass of clay in composite was established in order to obtain composite clay: HAP at 1:1 ratio, assuming 85% yield of HAP synthesis). The flask was heated in a water bath at temperature of 100°C, flask content was stirred mechanically. Next, within an hour,

0.15 dm³ of 0.06 mol/dm³ calcium acetate solution and 0.15 dm³ of 0.10 mol/dm³ potassium hydrogen phosphate solution, were dropped into the flask. Afterwards, the suspension was kept boiling for an hour. After that, the mixture was cooled down, sediment was decanted and washed with redistilled water. HAP-clay composite was dried at 80°C for 24 hours. In the same way (using wet method) pure hydroxyapatite was also prepared.

To estimate the textural characteristics of the samples (Table 1), low-temperature (77.4 K) nitrogen adsorption–desorption isotherms were recorded using a Micromeritics ASAP 2405 adsorption analyzer.

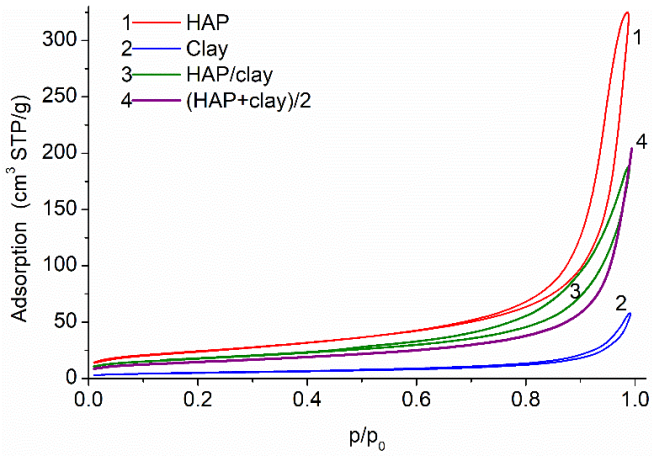

Fig. 1. Nitrogen adsorption-desorption isotherms of the materials studied (curves 1-3) and a sum of the isotherms for HAP and clay (curve 4) showing some non-additivity of the materials in the blend (curve 3)

The surface area (Table 1, S_{BET}) was calculated according to the BET method (Gregg and Sing, 1982). The total pore volume (Table 1, V_p) was evaluated from the nitrogen adsorption at $p/p_0 \approx 0.98$-0.99, where p and p_0 are the equilibrium and saturation pressure of nitrogen at 77.4 K, respectively (Adamson and Gast, 1997). The nitrogen desorption data were used to compute the pore size distributions (PSD, differential $f_V(R) \sim dV_p/dR$ and $f_S(R) \sim dS/dR$) using a self-consistent regularization (SCR) procedure (Gun'ko, 2014) under non-negativity condition ($f_V(R) \geq 0$ at any pore radius R) at a fixed regularization parameter $\alpha = 0.01$ (Provencher, 1982) (Fig. 3). A complex pore model was applied with slit-shaped (S) and cylindrical (C) pores and voids (V) between spherical NPNP (silica or/and alumina) packed in random aggregates (SCV/SCR method) (Gun'ko, 2014). The differential PSD with respect to the pore volume $f_V(R) \sim dV/dR$, $\int f_V(R)dR \sim V_p$ were re-calculated to incremental PSD (IPSD) at $\Phi_V(R_i) = (f_V(R_{i+1}) + f_V(R_i))(R_{i+1} - R_i)/2$ at $\sum\Phi_V(R_i) = V_p$). The $f_V(R)$ and $f_S(R)$ functions were also used to calculate contributions of nanopores (V_{nano} and S_{nano} at radius in the range 0.35 nm < R < 1 nm), mesopores (V_{meso} and S_{meso} at 1 nm < R < 25 nm), and macropores (V_{macro} and S_{macro} at 25 nm < R < 100 nm) (Gun'ko, 2014). For evaluation of deviation (Δw) of the pore shape from the model, a parameter

$$\Delta w = S_{BET} / \int_{R_{min}}^{R_{max}} f_s(R)dR - 1 \quad (1)$$

where R_{max} and R_{min} are the maximal and minimal pore radii, respectively, may be used as a criterion of the reliability of the pore model, since S_{BET} is a conventional parameter independent of the pore shape and material type. The average values of the pore radii were determined with respect to the pore volume ($X = V$) and the surface area ($X = S$), respectively, as the corresponding moments of the distribution functions

$$\langle R_X \rangle = \int_{R_{min}}^{R_{max}} R f_X(R)dR / \int_{R_{min}}^{R_{max}} f_X(R)dR. \quad (1)$$

Infrared spectra were registered by means of the FTIR spectrometer Nicolet 8700A with the attachement smart Orbit TR diamond ATR. Studies of X-ray diffraction (XRD) radiation diffraction were carried out using a diffractometer Empyrean PANalytical (lamp CULEF HR, detector-pixcel-3D, active canals 255).

Measurement of grain distribution was made using the Mastersizer 2000 apparatus produced by Malvern Instruments Ltd. with the hydro 2000 unit (A). 50 cm³ of suspension containing 0.05 g sample

was placed in the apparatus cell. During the measurement the rate of suspension flow through the measuring cell adjusting the pump revolutions and ultrasound intensity, was chosen.

Zeta potential measurements using NaCl solution in the concentration of 10^{-1}, 10^{-2}, 10^{-3} mol/dm^3 were made using the Zetasizer Nano-ZS apparatus produced by Malvern Instruments Ltd. In the zeta potential calculations the Smoluchowsky's equation was applied because of κa~150. 0.05 g of adsorbent was added to the solution of a given concentration and subjected to dispersion using the ultrasound probe Sonicator XL 2020 produced by Misonix. Then the suspension was poured into 0.125 dm^3 flasks, and pH was established to be 2-12 using 0.1M HCl and NaOH solutions. Six measurments of zeta potential were made fo each solution and the obtained results are presented in the form of diagrams.
Potentiometric titration was carried out using NaCl solutions in concentration of 0.001 mol/dm^3 for oxides and 0.001 mol/dm^3 for HAP, white clay and composites. The measurements were performed simultaneously for suspensions of the same solid content to keep the identical conditions of the experiments in a thermostated Teflon vessel at 25°C. To avoid the influence of CO_2, all potentiometric measurements were performed under the nitrogen atmosphere. pH values were measured using a set of glass REF 451 and calomel pHG201-8 electrodes with the Radiometer assembly. The surface charge density was calculated from the difference of the amount of acid or base added to obtain the same pH value of suspension as for the background electrolyte.

3. Results and discussion

3.1. Structural and textural characterization

The textural characteristics (Table 1) show that the studied samples having different surface area (S_{BET} and S components) and pore volume (V_p and V components) are rather mesoporous since mesopores give the main contributions to these characteristics.

Table 1. Textural chracteristics of HAP, white clay and composite white HAP/clay

Parameter	HAP	White clay	White clay/HAP
S_{BET} (m^2/g)	86	18	63
S_{nano} (m^2/g)	3	2	3
S_{meso} (m^2/g)	71	14	55
S_{macro} (m^2/g)	12	2	5
V_p (cm^3/g)	0.509	0.093	0.295
V_{nano} (cm^3/g)	0.002	0.001	0.002
V_{meso} (cm^3/g)	0.325	0.048	0.209
V_{macro} (cm^3/g)	0.182	0.044	0.084
$<R_V>$ (nm)	24.44	28.98	21.68
$<R_S>$ (nm)	13.21	9.80	9.15
Δw	0.245	-0.052	0.208
c_{slit} (arb. un.)	0.073	0.388	0.264
c_{cyl} (arb. un.)	0.892	0.285	0.443
c_{void} (arb. un.)	0.035	0.327	0.293

Note. Contributions of nano- (V_{nano} and S_{nano}), meso- (V_{meso} and S_{meso}), and macropores (V_{macro} and S_{macro}) were calculated by integration of the $f_V(R)$ and $f_S(R)$ functions at 0.35 nm < R_{nano} < 1 nm, 1 nm < R_{meso} < 25 nm, and 25 nm < R_{macro} < 100 nm, respectively. $<R_V>$ and $<R_S>$ are the average pore radii calculated as a ratio of the first moment of $f_V(R)$ or $f_S(R)$ to the zero moment (integration over the 0.35-100 nm range) $<R> = \int f(R)RdR/\int f(R)dR$; c_{slit}, c_{cyl}, and c_{void} are the weight constants and Δw is the deviation of the pore shape from the model calculated using the SCV/SCR method.

The composite preparation results in a certain non-additivity of the textural characteristics (Table 1, Figs. 1 and 2) due to precipitation of HAP layers onto clay particles that enables formation of smaller HAP particles bonding to clay particles than those for HAP alone. For example, the nitrogen adsorption isotherm for the composite is located over the normalized sum of the isotherms for HAP and clay alone (Fig. 1). The IPSD for the blend (Fig. 2, curve 3) is greater than that of components alone (curves 1 and

2) at 4 nm < R < 10 nm. However, for V_p and V_{macro} (Table 1), there is the opposite result in contrast to V_{meso}. These changes are correlated to changes in the $<R_V>$ and $<R_S>$ values, which are smaller for the composite due to changes in the condition of the HAP particle formation with the presence of clay particles.

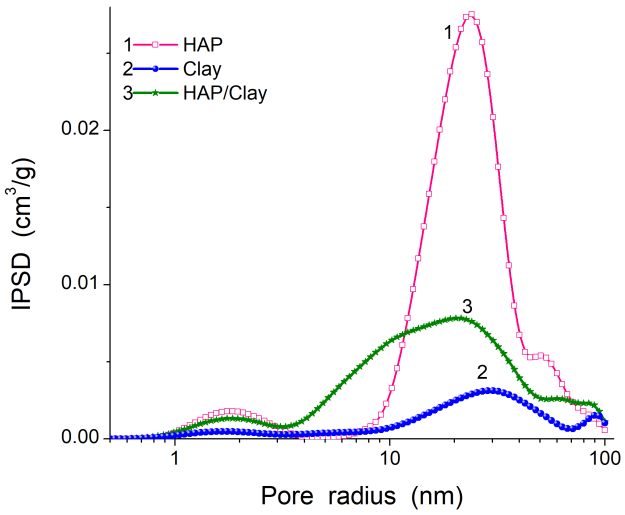

Fig. 2. Incremental pore size distributions for the materials studied (SCV/SCR method)

The white clay sample is crystalline and the composite is crystalline too and contains both crystalline phases. Crystalline structure was analyzed using XRD method recording patterns at 2θ = 10–80° (Fig. 3). Comparison of the obtained patterns with the ASTM database shows that hydroxyapatites are crystalline in individual HAP (the peaks characteristic for the crystalline form of HAP are evidenced by the following 2θ values and corresponding intensities: 25.9–100%, 32.96–55%, 39.84–20%; 46.7–40%, and 49.5–30%), as well white clay as crystallite kaolinite $Al_4(OH)_8Si_4O_{10}$ with admixtures of muscovite, rutile, dickite and illite. Composite has the peaks characteristic for hydroxyapatite, kaolinite and dickite. This structure of the composite can be favorable for some applications as a biomaterial.

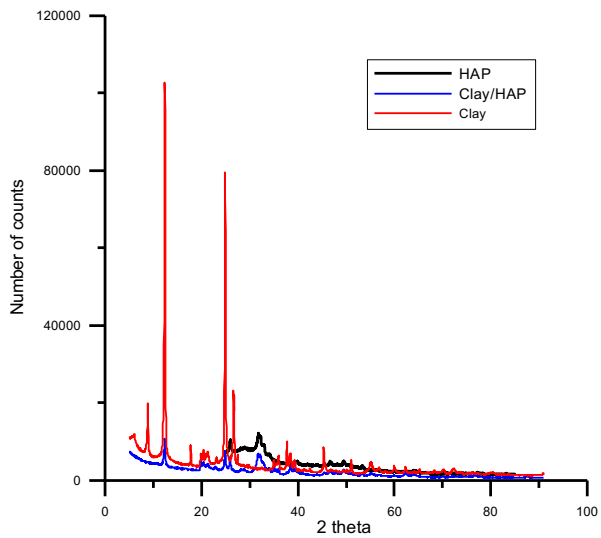

Fig. 3. XRD pattern of white clay, hydroxyapatite and composite white clay/HAP

Table 2. Values of diameters (μm) characterizing adsorbent agglomerates distribution

	HAP	White clay /HAP	White clay
d (0.1) μm	1.49	0.50	2.53
d (0.5) μm	1.56	0.62	3.76
d (0.9) μm	8.02	2.12	6.25

Table 2 presents the values of grain diameters of the materials studied. The obtained results indicate that there are mainly aggregates of nanoparticles and agglomerates of aggregates, which can be crushed using eg. ball milling. The values of the coefficient d (0.1), specifying a particle size of 10% of the total number, d (0.5), describing the mean value of the measured particles and d (0.9), which is 90% of the total number of particles, show that the obtained composites have less grain size than their ingredients. The exact characteristics of the system under consideration in terms of grain size is very important when interpreting electrochemical results, especially the zeta potential, hence very often research is carried out on well-defined model systems.

According to FTIR spectra, the stretching bands at 3571 cm^{-1}, vibrations bands at 635 cm^{-1} originating from OH−groups, as well characteristic bands due to PO_3^{-4} ions are clearly visible. Figure 4 shows a typical spectrum for hydroxyapatite, showing PO_3^{-4} derived bands at 565, 603, 962 and 1033 cm^{-1}. All these modes are Raman and infrared active and observed for all the spectra. Some CO_3^{-2} derived bands are observed at 873, 1420, and 1480 cm^{-1}. A broad band in the range of 3700–3000 cm^{-1} is the O-H stretching vibrations of sorbed water. The well resolved vibration band at 3570 cm^{-1} indicates the presence of isolated and twin O-H groups from the hydroxyapatite structure (Rapacz-Kmita et al., 2005). For white clay, main IR bands are related to the stretching vibrations of the bonds Al–O, Si–O, Al–O–Si (ν < 1200 cm^{-1}), AlO–H (hydroxyl groups at the interlayer surface (see Fig. 4) at ν_{OH} = 3695 and 3620 cm^{-1} and less intensive band at 3656 cm^{-1}), SiO–H in kaolinite defects and at a quartz surface (3000 cm^{-1} < ν_{OH} < 3750 cm^{-1}).

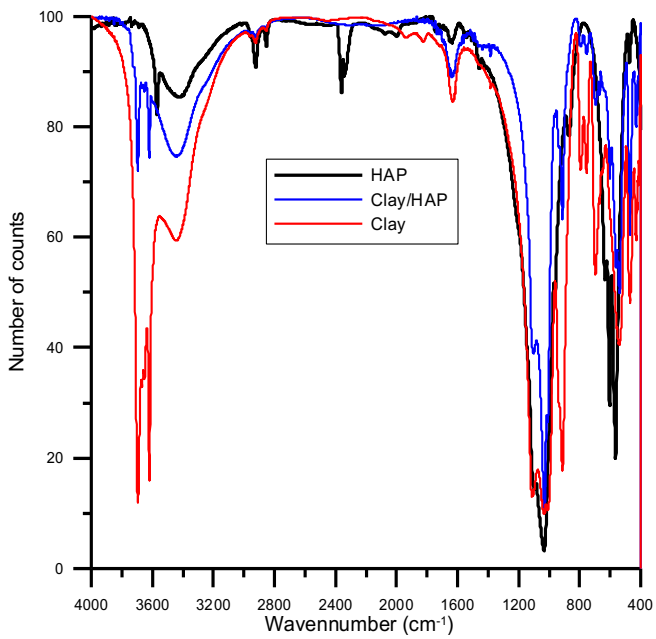

Fig. 4. FTIR spectra of HAP, white clay and composite white clay/HAP

3.2. Electrochemical characterization

The electrokinetic behavior of particles in the aqueous suspensions is extremely important in determining their stability and rheological properties. The zeta potential plays an important role in determining the stability of clays and their composites in aqueous solutions that are usually susceptible to aggregation. The stability and rheological properties of alumina slurries and their composites are important in the production of technologically advanced cosmetics.

Tabel 3. Electrokinetic parameters

Adsorbent	pH_{pzc}	pH_{IEP}
HAP	7.9	<4
White clay	7.30	<2
White clay/ HAP	8.95	<2

Potentiometric titration is the most frequently applied method to determine the point of zero charge (PZC) in the adsorbent/electrolyte solutions. The important parameters characterizing the electrical double layer (EDL) is pH_{PZC}. The latter is the point in which the concentration of positively charged surface groups is equal to the concentration of negatively charged groups. For samples studied (Table 3), due to the effect of HAP deposits onto clay particles, higher pH_{PZC} for the composite than for white clay and hydroxyapatite, was noted. When the amount of positive and negative charges in the diffuse layer of the EDL are equal to each other, it is called the isoelectric point (IEP) of the solid surface (pH_{IEP}). Then the resultant charge of the diffuse layer of the EDL is zero. Due to the fact that the concentration of potential-forming ions (H^+ and OH^-) depends on the pH of the solution, therefore the pH_{IEP} point corresponds to a precisely determined pH value. pH_{IEP} of all tested powders, i.e. white clay, white clay/HAP composites, are below pH 2 and for HAP <4.

The systems studied have the highest absolute values of the zeta potential for the lowest electrolyte concentration and the lowest absolute values for the highest electrolyte concentration (Fig. 5). It was found that the zeta potential decreased with increasing electrolyte concentration, which results from the dissociation of surface groups to ionization on white clay and it's composite with HAP. In the examined systems, we also observed that the zeta potential decreases with increasing pH. An important quantum of the dispersed particles in the liquid is the colloidal stability, i.e. the ability of the particles to remain in the form of a colloidal dispersion. Dispersions that are unstable may undergo coagulation or sedimentation processes, the consequence of which is the delamination of the sample. Quantity can be used to quantify the dispersion stability. It is assumed that the dispersion is stable for an absolute value of zeta potentials > 30mV. The zeta potential for the tested samples in the tested pH ranges from 2 to 12 and electrolyte concentrations ranges from 0 mV to -45 mV, i.e. in the majority of the ranges tested, the selected systems are unstable in the colloidal form, they may be delaminated. Stable systems, is when the absolute potential value is lower than 30 mV, we obtained only for the following samples: white clay/0.001 mol/dm^3 at pH 8, 10, 12; HAP and all tested electrolytes at pH> 10. Comparison of results for pure white clay and its composites with HAP shows that at the same electrolyte concentrations similar absolute values of zeta potential are noted, and differs from pristine hydroxyapatite. As a result, the surface potential of white clay exerts the main impact on the zeta potential.

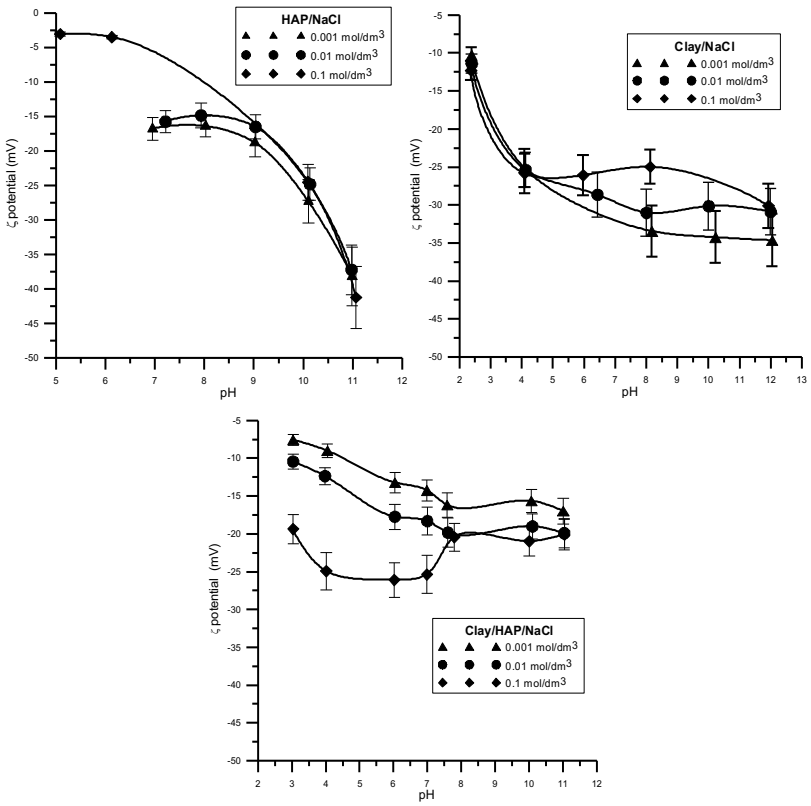

Fig. 5. Dependence of ζ potential as the pH function in NaCl solutions for: (a) HAP, (b) white clay and (c) white clay/HAP

The comparison of pH_{PZC} and pH_{IEP} position indicates that pH_{IEP} is shifted by about 3 units toward the acidic side. A similar shift was found for the systems in which adsorption of specific ions proceeds. In the case of basic electrolyte, a similar situation can occur for the porous systems characterized by energetic heterogeneity of a surface. The studied samples belong to the systems characterized by the textural porosity. The pores can be ''clogged'' during electrophoresis measurements, and the properties of this part of solid is not disclosed. Therefore, a large part of charge can be compensated inside textural pores (voids between nanoparticles in aggregates) of aggregates and only a part raising from the ionized groups on the outer surface of secondary particles is responsible for the electrophoretic mobility.

4. Conclusions

The composite with hydroxyapatite/kaolinite clay was prepared using white clay as a matrix upon hydroxyapatite precipitation with the reaction of Di-potassium hydrogen phosphate (K_2HPO_4). Studies of the crystalline structure of the composites applying XRD method showed the presence of crystalline hydroxyapatite and white clay phases. The precipitation of HAP onto clay particles changes the HAP formation conditions in comparison to the formation of HAP alone. This difference affects the textural characteristics of the materials that demonstrate certain non-additivity. The values of pH_{pzc} and pH_{IEP} characterizing the EDL depend on the type of the white clay matrix. Comparative studies of HAP, white clay and composites using adsorption and desorption of nitrogen, and FTIR showed that in most cases composites have properties intermediate between hydroxyapatite and the white clay taken for the synthesis.

References

ADAMSON, A.W., GAST, A.P., 1997. *Physical chemistry of surface*, Sixth edition. Wiley, New York.

BERGAYA, F., THENG, B.K.G., LAGALY, G. (Eds.), 2006. *Developments in clay science*. Handbook of Clay Science. Elsevier, Amsterdam. ISBN: 9780080441832, 9780080457635.

DEAN-MO, L., 1996. *Fabrication and characterization of porous hydroxyapatite granules.* Biomaterials 17, 1955-1957.

DOROZHKIN, S.V., 2010. *Nanosized and nanocrystalline calcium orthophosphates.* Acta. Biomater. 6, 715-735.

EBERL, D.D., FARMER, V.C., BARRER, R.M., 1984. *Clay mineral formation and transformation in rocks and soils*. Phil. Trans. R. Soc. Lond. A 311, 241–257.

EHLERS, E.G., BLATT, H., 1982. *Petrology, igneous, sedimentary, and metamorphic*. W.H. Freeman & Co, San Francisco.

GREGG, S.J., SING, K.S.W., 1982. *Adsorption, surface area and porosity*. Academic Press, London.

GUGGENHEIM, S., 1995. *Definition of clay and clay mineral: Joints report of the AIPEA nomenclature and CMS*. Nomenclature Committees. Clay Minerals.

GUN'KO, V.M., 2014. *Composite materials: textural characteristics*. Appl. Surf. Sci. 307, 444–454.

GUZMAN, V.C., PINA, B.C., MUNGUIA, N., 2005. *Stoichiometric hydroxyapatite obtained by precipitation and sol gel processes.* Rev. Mex. Fis. 51, 284 -293.

HILLIER, S. 2006. *Formation and alteration of clay materials*. In: Reeves, G.M. & Cripps, J.C. (Eds) Clays Materials Used in Construction. Geological Society, London, Engineering Geology Special Publications, 21, 29–71.

ITO, A., WAGAI, R., 2017. *Global distribution of clay-size minerals on land surface for biogeochemical and climatological studies.* Scientific Data 4, Article number 170103.

JANUSZ, W., SKWAREK, E., 2016. *Study of sorption processes of strontium on the synthetic hydroxyapatite.* Adsorption 22, 697-706.

KENNE DEDZO, G., DETELLIER, C., 2017. *Characterization and applications of kaolinite robustly grafted by an ionic liquid with naphthyl functionality.* Materials 10, 1006-1018.

MIDDLETON, G.V., CHURCH, M.J., CONIGLIO, M., HARDIE, L.A., LONGSTAFFE, F.J. (Eds.), 2003. *Encyclopedia of sediments and sedimentary rocks*. Kluwer Academic Publishers, Dordrecht.

MIRANDA-TREVINO, J.C., COLES, C.A., 2003. *Kaolinite properties structure and influence of metal retention on pH.* Appl. Clay Sci. 23, 133-139.

MISHRA, G., DASH, B., PANDEY, S., 2018. *Layered double hydroxides: A brief review from fundamentals to application as evolving biomaterials.* Appl. Clay Sci. 153, 172–186.

MONTES-HERNANDEZ, G., FINDLING, N., RENARD, F., AUZENDE, A.-L., 2014. *Precipitation of ordered dolomite via simultaneous dissolution of calcite and magnesite: New experimental insights into an old precipitation enigma*. Cryst. Growth Des. 14, 671-677.

MOSTAFA, N.Y., 2005. *Characterization, thermal stability and sintering of hydroxyapatite powders prepared by different routes*. Mater. Chem. Phys. 94, 333-341.

MURUGAN, R., RAMAKRISHNA, S., 2007. *Development of cell-responsive nanophase hydroxyapatite for tissue engineering*. Amer. J. Biochem. Biotechn. 3, 118-124.

MURRAY, H.H., 1991. *Overview - clay mineral applications*. Appl. Clay Sci. 5, 379-395.

PROVENCHER, S.W., 1982. *A constrained regularization method for inverting data represented by linear algebraic or integral equations*. Comp. Phys. Comm. 27, 213-227.

RAPACZ-KMITA, A., PALUSZKIEWICZ, C., SLÓSARCZYK, A., PASZKIEWICZ, Z., 2005. *FTIR and XRD investigations on the thermal stability of hydroxyapatite during hot pressing and pressureless sintering processes*. J. Mol. Struct. 744-747, 653-659

RHEE, S.H., 2002. *Synthesis of hydroxyapatite via mechanochemical treatment*. Biomaterials 23, 1147-1152.

RIMAN, R.E., SUCHANEK, W.L., BYRAPPA, K., WEI CHEN, C., SHUK, P., OAKES, C.S., 2002. *Solution synthesis of hydroxyapatite designer particulates*. Solid State Ionics 151, 393-402.

SKWAREK, E., JANUSZ, W., STERNIK, D., 2017. *The influence of the hydroxyapatite synthesis method on the electrochemical, surface and adsorption properties of hydroxyapatite*. Adsorp. Sci. Technol. 35, 507-518.

SKWAREK, E., JANUSZ, W., 2016. *Adsorption of Cd (II) ions at the hydroxyapatite/electrolyte solution interface*. Sep. Sci. Technol. 51, 11-21.

SOBCZAK, A., KOWALSKI, Z., WZOREK, Z., 2009. *Preparation of hydroxyapatite from animal bones*. Acta Bioeng. Biomech. 11, 23-28.

SOPYAN, I., SINGH, R., HAMDI, M., 2008. *Synthesis of nano sized hydroxyapatite powder using sol-gel technique and its conversion to dense and porous bodies*. Indian J. Chem. 47, 1626–1631.

SUZUKI, S., OHGAKI, M., ICHIYANAGI, M., OZAWA, M., 1998. *Preparation of needle-like hydroxyapatite*. J. Mater. Sci. Lett. 17, 381-383.

SZYMAŃSKI, A., 1991. *Biomineralisation and biomaterials*. State Publishing House Warsaw, Poland.

ZHANG, J., ZHOU, C.H., PETIT, S., ZHANG, H., 2019. *Hectorite: Synthesis, modification, assembly and applications*. Appl. Clay Sci. 177, 114–138.

ZHUANG, G., ZHANG, Z., JABER, M., 2019. *Organoclays used as colloidal and rheological additives in oil-based drilling fluids: An overview*. Appl. Clay Sci. 177, 63–81.